

Controllable self-assemblies of micro/nano-tubes and vesicles from arylamides and their applications as templates to fabricate Pt micro/nano-tubes and hollow Pt nanospheres†

Yun-Xiang Xu, Gui-Tao Wang, Xin Zhao,* Xi-Kui Jiang and Zhan-Ting Li*

Received 26th August 2009, Accepted 7th December 2009

First published as an Advance Article on the web 18th January 2010

DOI: 10.1039/b917576h

A novel class of nonamphiphilic aromatic amides (**T1–T3**) have been designed and synthesized from naphthalene-2,7-diamine or 2-amino-naphthalene and a 5-hydroxy-isophthalic acid segment, which is revealed to selectively assemble into vesicular or tubular architectures, depending on the solvents and concentrations. **T1** and **T2** form vesicles in methanol, but can be converted into micro/nano-tubes when water is added and further gelate the binary solvent when the concentration is high enough. In contrast, **T3** self-assembles into fine tubular structures in methanol, but can be transformed into vesicles upon being diluted or adding chloroform. The morphology transition has been investigated by SEM, AFM, TEM and fluorescent microscopy, which also reveal that microtubes of large size are formed through the fusion of vesicles of small size, which is driven by the cooperative hydrogen bonding and aromatic stacking interactions, as evidenced by the X-ray investigation on an analogue of **T3**. The novel organic micro/nano-tubes and vesicles are further used to template the fabrication of Pt micro/nano-tubes or hollow Pt spheres by *in situ* reduction of the absorbed K_2PtCl_4 with ascorbic acid, as confirmed by SEM, TEM and EDX analyses.

Introduction

The self-assembly of low-molecular-weight organic molecules has drawn considerable attention in the past decade for its powerful applications in fabricating nano- and microscale objects.^{1,2} In such a process, small molecules are drawn together by noncovalent interactions, such as hydrogen bonding, aromatic stacking and van der Waals interactions, resulting in the formation of discrete ordered complex structures. As basic building blocks for this “bottom-up” approach, organic compounds have advantages of structural variety, ready modifications and multifunctionality. Based on this strategy, a variety of well-defined nanoscale structures, including vesicles,^{3–7} nano-tubes,^{8–12} and nanofibers,^{13–15} have been constructed.

Owing to the intrinsic features of noncovalent interactions such as reversibility and sensitive response to external stimuli and weak binding strength, one crucial challenge in organic molecular self-assembly is the selective formation of specific assembled targets in solution or on surfaces. To reach this goal, rational design and modification of the self-assembling building blocks at the molecular level have been the most widely adopted approach.^{16–20} In addition to structural modification, changing the environmental conditions such as pH,^{21,22} temperature,^{23,24}

concentration,^{25–27} and polarity of the medium^{28,29} have also been explored to offer efficient control over the self-assembling process. This approach is attractive because different architectures may be assembled from the identical building blocks. Herein we report a novel class of aromatic amide-based non-amphiphiles that can self-assemble into vesicular and tubular structures by simply changing the solvents and/or concentrations. In addition, the new assembled architectures have been further utilized to template the formation of fine Pt micro/nano-tubes and hollow Pt spheres, the preparation of which was mainly limited to an inorganic template approach.^{30–36}

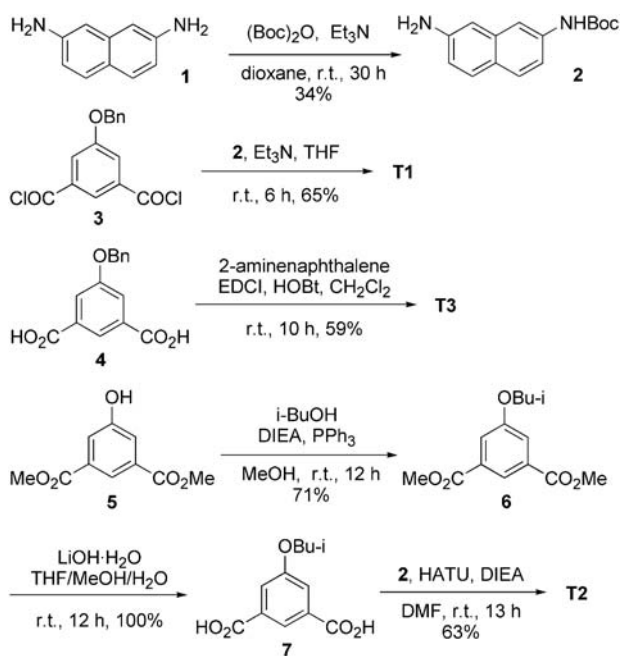
Results and discussion

Design and synthesis

We have previously reported a series of amphiphilic aromatic amide oligomers that are capable of self-assembling into vesicular structures in methanol.³⁷ Since vesicles have been mainly constructed from amphiphilic molecules, such as surfactants and lipids, and copolymers,^{38–42} and the fabrication of vesicular structures from nonamphiphilic compounds are quite rare,^{43–45} we therefore further designed and synthesized a new class of non-amphiphilic aromatic amides, *i.e.*, **T1–T3**, to explore their capacity of forming vesicular structures. The synthesis of **T1–T3** is straightforward. For the preparation of **T1**, diamine **1** was first reacted with di-*tert*-butyl dicarbonate to afford **2** in 34% yield, which was then reacted with diacyl chloride **3** to give **T1** in 65% yield, while **T3** was prepared from the coupling reaction of diacid **4** with 2-amino-naphthalene. For the synthesis of **T2**, compound **5** was first treated with iso-butanol to afford **6** in 71% yield. The diester was further hydrolyzed with lithium hydroxide to give **7**

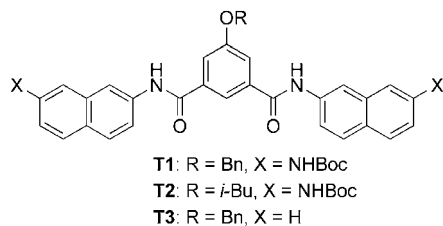
State Key Lab of Bioorganic and Natural Products Chemistry, Shanghai Institute of Organic Chemistry, Chinese Academy of Sciences, 345 Lingling Lu, Shanghai 200032, China. E-mail: xzhao@mail.sioc.ac.cn; ztli@mail.sioc.ac.cn; Fax: +0086-21-64166128; Tel: +0086-21-54925122

† Electronic supplementary information (ESI) available: Experimental details, synthesis and characterization, fluorescent micrographs, AFM image, additional SEM and TEM images, and XRD result. CCDC reference number 715335. For ESI and crystallographic data in CIF or other electronic format see DOI: 10.1039/b917576h



Scheme 1 The synthetic routes for compounds **T1**–**T3**.

quantitatively. The diacid was then coupled with **2** to yield **T2** in 63% yield (Scheme 1).



Self-Assembly properties in methanol

The self-assembly of **T1**–**T3** were first investigated in methanol. Morphologies of the aggregates of **T1**–**T3** were characterized by SEM, which revealed that **T1** and **T2** self-assembled into spherical structures. The sizes of the spheres formed by them were comparable, with an average of 2 μm in diameter. Compared to those of **T2**, the spheres formed from **T1** showed a little tendency of fusing (Fig. 1a and 1b). Under similar conditions, **T3**, which has no NHBoc groups at the ends of the backbone, gave rise to fine tubular microstructures when the concentration was 1 to 5 mM (Fig. 1c and Fig. S1 of ESI[†]). The hollow nature of the tubes was evidenced by their open-ended feature. Upon being diluted to 0.5 or 0.2 mM, tubular structures could not be observed. Instead, spheres much smaller than those of **T1** and **T2** were generated exclusively (Fig. 1d and Fig. S1 of ESI[†]). Similar conversions were reported previously for peptide-based nanotubes and attributed to the collapse of compact stacking structures of the tubes into less compact stacking vesicular structures.^{46–48} No similar tubular structures were observed for **T1** and **T2**. Moreover, their spherical morphology almost did not change even when the concentration was decreased to 0.01 mM (*vide infra*, Fig. 2).

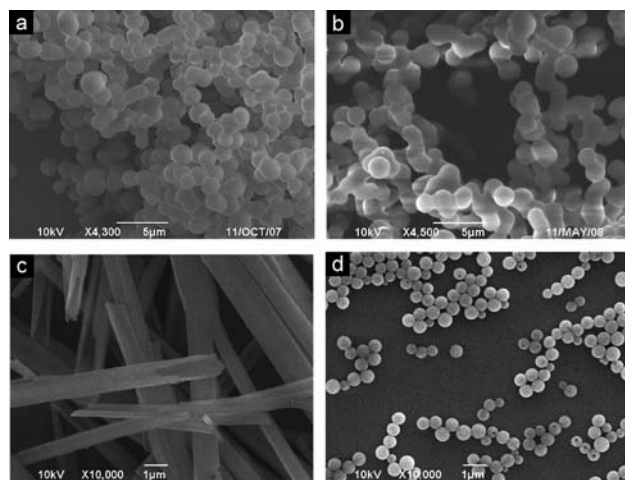


Fig. 1 SEM images of (a) **T1** (5 mM), (b) **T2** (5 mM), (c) **T3** (2 mM), and (d) **T3** (0.2 mM) on silicon surface. The samples were obtained by evaporation of the methanol solutions.

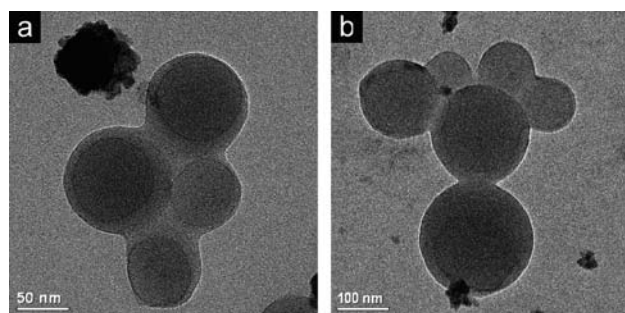


Fig. 2 TEM images of (a) **T1** and (b) **T2**. The samples were obtained from their methanol solution (0.01 mM).

AFM images showed that the spherical aggregates of **T1** had a large ratio of diameter over height (*ca.* 13.2, Fig. S2 of ESI[†]), which might be attributed to hollowness of the spheres or the high local force applied by the AFM tip.⁴⁹ The hollow feature of the spheres was further evidenced by TEM (Fig. 2), which showed a contrast between the inner part and the periphery.⁵⁰ The wall thickness was estimated to be *ca.* 2.5 and 2.6 nm for **T1** and **T2**, respectively, which is close to the length of their extended backbone (*ca.* 2.7 nm). Therefore, the wall of the vesicles might be generated by a monolayered stacking of the molecules with the Boc groups being located outside.

Effect of the solvent polarity on the assembling selectivity

Experiments in the methanol–water binary solvent were carried out to investigate the effect of the solvent polarity on the assembling behavior of **T1**–**T3**. It was found that in this more polar media **T1** and **T2** self-assembled into tubular structures, as evidenced by SEM, TEM and fluorescent microscopy images (Fig. 3 and Fig. S3 of ESI[†]). Moreover, they could further gelate the solvent at higher concentrations. The minimum gelation concentrations were 1.09 and 1.77 wt%, respectively, for the methanol–water system (5 : 1, v/v). SEM images showed that the gels of both compounds were generated by hollow tubes of

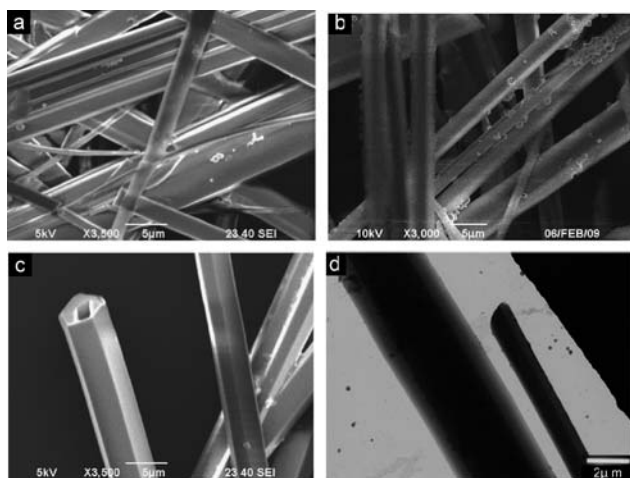


Fig. 3 (a) SEM image of **T1**, (b) SEM image of **T2**, (c) SEM image of **T3** and (d) TEM image of **T1** (80 kV). The samples (5 mM) were obtained from methanol–water (5 : 1).

several micrometres in width and dozens of micrometres in length (Fig. S4 of ESI†). Attempts to measure the wall thickness of the hollow tubes by high resolution TEM was not successful because the tubular structures could not survive the condition used (200 kV). Different from **T1** and **T2**, **T3** exclusively formed tubular microstructures, independent of the methanol–water ratio.

The assembling behavior in the methanol–chloroform binary solvent was also investigated (Fig. 4 and Fig. S5 of ESI†). When the content of chloroform was $\leq 10\%$, **T1** (5 mM) gave rise to vesicles exclusively (Fig. 4a). When the content was increased to 25%, SEM images did not show any vesicular structures. In pure chloroform, **T1** formed belt-like aggregates. Their salient feature was illustrated by the twisted belt in the middle of the SEM image shown in Fig. 4b. **T2** showed a similar trend. However, in pure chloroform no well-defined aggregates were generated. Adding chloroform also strongly induced **T3** (2 mM) to form vesicular structures. Thus, in the presence of 10% of chloroform, **T3** could form vesicles selectively (Fig. 4d). The vesicles retained their structure even when the content of chloroform was increased to 50%. Increasing the concentration facilitated the formation of the tubular structures. For example, the solution of 5 mM still selectively formed microtubes even when 25% of chloroform was added. Further increasing the content of chloroform gradually destroyed these well-ordered tubular structures. Interestingly, microtubes could be generated again in pure chloroform (Fig. 4f). It should be noted that the cross sections of the resulting tubes are not exclusive. For example, while tubes with a hexagon-like section were observed in methanol–water (5 : 1) as shown in Fig. 3c, microtubes with a rectangular cross section were also obtained (Fig. S6a of Supporting Information) from the same sample. In addition, microtubes with hexagon-like section and rectangular section were observed for a sample prepared from methanol–chloroform (3 : 1) (Figures S 6b–c of ESI†), besides the squared section illustrated in Fig. 4e. However, the reason for the formation of such cross sections is yet unclear. In nonpolar decalin, **T1** and **T2** also formed spherical structures, while **T3** produced tubular aggregates

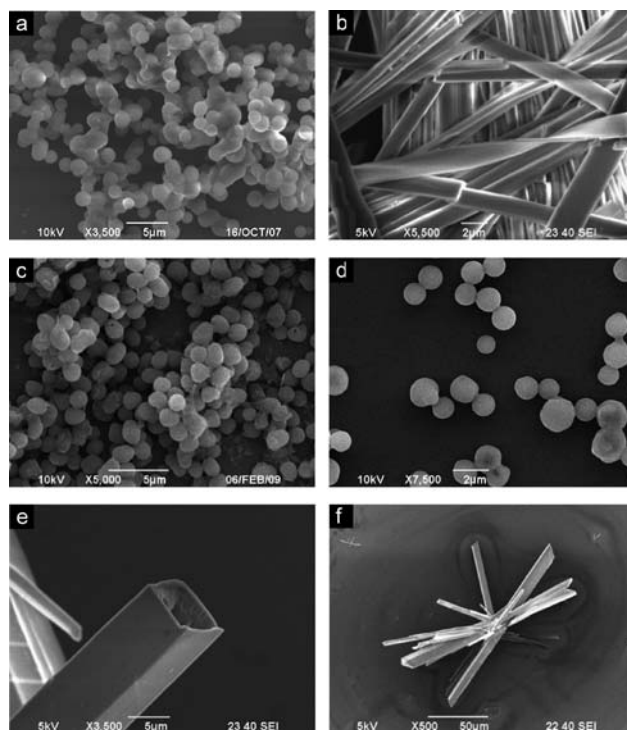


Fig. 4 SEM images of (a) **T1** (5 mM) from methanol–chloroform (9 : 1), (b) **T1** (5 mM) from chloroform, (c) **T2** (5 mM) from methanol–chloroform (9 : 1), (d) **T3** (2 mM) from methanol–chloroform (9 : 1), (e) **T3** (5 mM) from methanol–chloroform (3 : 1) and (f) **T3** (5 mM) from chloroform.

(Fig. S7 of ESI†). These results were similar to those in polar methanol, suggesting that **T1–T3** might adopt similar packing modes in the two solvents.

Self-assembling mechanism

The assembling process of **T1–T3** should be driven by cooperative intermolecular hydrogen bonding and aromatic stacking interactions.³⁷ The IR spectra of their dried samples of the tubes, obtained after the solvent was removed, exhibited the N–H stretching vibrations around 3290 cm^{-1} , indicating that the amide proton was engaged in intermolecular H-bonding. The benzyl or iso-butyl units should also contribute significantly, serving as “glue” or an “anchor” to crosslink the stacking layers, because compound **T4** (Fig. 5), which lacks such units, did not form any ordered microstructures under the above conditions. Attempt to grow single crystals of **T1–T3** suitable for the X-ray crystallography was not successful. However, the crystal structure of **T5**† (Fig. 5), an analog of **T3**, revealed that the neighboring molecules were packed with each other in oppositely alternate manner stabilized by two pairs of $\text{C}=\text{O}\cdots\text{H}-\text{N}$ hydrogen bonds, even though the appended benzyl group was

† Crystal data for **T5**: $\text{C}_{27}\text{H}_{22}\text{N}_2\text{O}_3$, $M = 422.47$, Monoclinic, space group $C2/c$, $a = 18.473(2)\text{ \AA}$, $b = 14.611(2)\text{ \AA}$, $c = 8.4322(12)\text{ \AA}$, $\alpha = 90.00$, $\beta = 103.972(4)$, $\gamma = 90.00$, $V = 2208.6(5)\text{ \AA}^3$, $T = 293(2)\text{ K}$, $Z = 4$, $D_c = 1.271\text{ g cm}^{-3}$, $\mu = 0.083\text{ mm}^{-1}$, $R_1 = 0.0822$, $wR_2 = 0.2481(I > 2\sigma(I))$, $R_{int} = 0.1027$, $wR_2 = 0.2460$ (all data). Reflections collected/unique: 5722/2050 ($R_{int} = 0.0848$). GOF = 1.073.

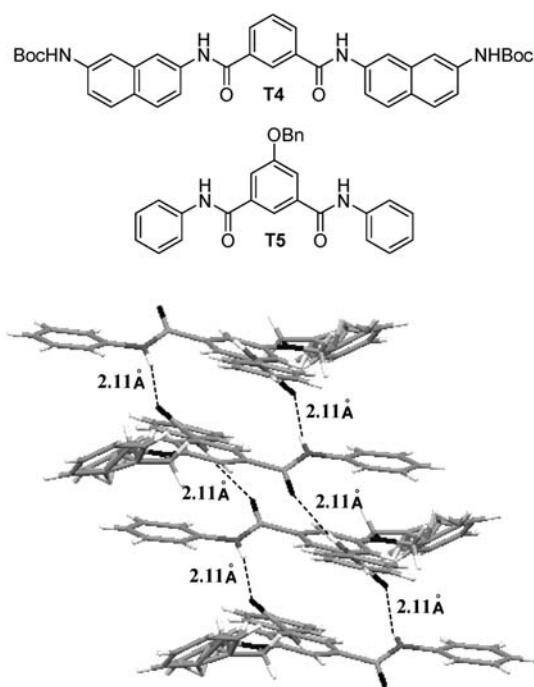


Fig. 5 The packing structure of **T5** in the crystal, highlighting the intermolecular hydrogen bonding and alternate stacking of the molecules. The appended benzyl unit is disordered due to two different orientation.

disordered in the crystal structure.⁵¹ **T5** could also self-assemble into tubular structures in methanol (Fig. S8 of ESI†). The powder XRD patterns of the nanotubes of **T5** were very close to the theoretical ones calculated from the crystal structure, indicating that the molecules in the tubes of **T5** adopted a similar packing mode as that in the crystal structure (Fig. S9 of ESI†). Therefore, we propose that the assembly of **T1–T3** was also driven by the two similar interactions. Moreover, their stacking interaction should be stronger than that of **T5** due to the existence of the two larger naphthalene units. Furthermore, compared to **T3**, **T1** and **T2** bear two NHBoc groups at their ends of the backbones, which can form two additional intermolecular hydrogen bonds. On the other hand, the steric hindrance imposed by the bulky Boc groups might push the monomers to align in a slightly twist arrangement, which should have influence on the self-assembling process and might improve the assembling selectivity by inhibiting the intermolecular head-to-tail contact.⁵²

A systematic SEM investigation of **T1** revealed that the tubular structures were generated through the time-dependent fusion of the smaller vesicles. For example, the sample of its freshly prepared methanol–water (20 : 1) solution (2 mM) showed that most vesicles fused into sheet-like structures, although there were some complete vesicles that could be observed (Fig. 6a). After the solution was incubated for 17 days at room temperature, most of these sheet-like structures evaluated into microtubes, on which some unconverted vesicles could also be found (Fig. 6b). This fusion process was also supported by the fluorescence microscopy study in methanol. However, in this case, the fusion took even longer time. As shown by Fig. 6c

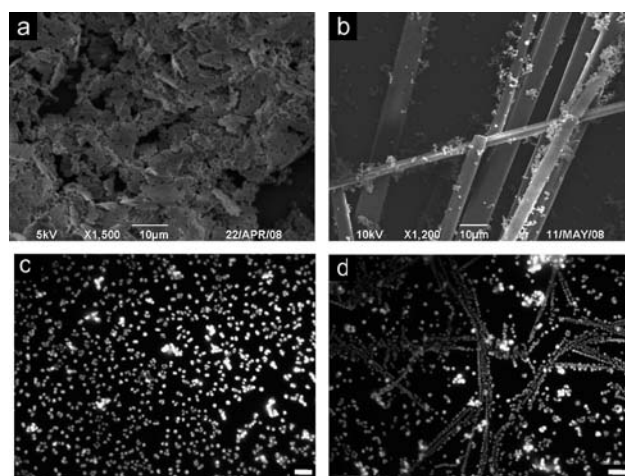


Fig. 6 SEM images of **T1** (2 mM) from methanol–water (20 : 1): (a) freshly prepared, (b) incubated for 17 days. Fluorescence microscopy images of **T1** (3 mM) from methanol of (c) freshly prepared and (d) incubated for 50 days. The scale bar for fluorescent images is 10 μm .

and 6d, freshly prepared sample from methanol gave rise to discrete spherical structures, which was consistent with the SEM observation. The spherical structures gradually connected each other to form necklace-like structures after 50 days (4 °C), which could further transform into tubes after another 42 days at room temperature. This result also indicated that the tubular structures were more stable than the vesicular structures and water accelerated the vesicle-tube transition by enhancing the stacking interaction. The powder XRD profiles of vesicles and tubes of **T1** exhibited almost identical patterns (Fig. S10 of ESI†), suggesting that both structures had a similar stacking pattern.⁵³

The conversion between vesicles and tubes should be a dynamic process.⁴⁷ As mentioned above, both IR and X-ray crystallography studies suggested that the self-assembling process was dictated by intermolecular hydrogen bonding and aromatic stacking interactions between the monomers. It is generally accepted that aromatic stacking is more favorable in higher polar solvents but hydrogen bonding becomes stronger in less polar solvent. Thus, the origin of the transition between vesicles and tubes might be ascribed to different dominating noncovalent interactions and a subtle balance of these interactions between the molecules in the solvents of different polarity. Aromatic stacking should be enhanced in the methanol–water binary solvent, which is proposed to be responsible for the formation of the tubular structures. For compound **T3**, aromatic stacking is more decisive than those of **T1** and **T2** because the latter two bear two more hydrogen-bonding sites. As a result, **T3** could self-assemble into tubular structures in methanol and even in chloroform (5 mM) while **T1** and **T2** could not under the same conditions.

Templates for Pt nanostructure

It has been established that the N and O atoms of amides have a high affinity towards Pt(II).⁵⁴ The O- and N-rich micro/nano-tubes and vesicles from **T1–T3** are therefore potentially useful in templating the fabrication of Pt micro/nano-tubes and spheres, if Pt(II) ions are anchored on their surface and further reduced to Pt(0) *in situ*.⁵⁵

T1 and **T3** were chosen to test this assumption, because the assembling objects from these two compounds were generally more stable. We started with the tubular template first as follows: to a 5 mM solution of **T1** in methanol–water (5 : 1), which had been confirmed to assemble into tubes, an aqueous solution of K_2PtCl_4 (20 mM, 0.1 mL) was added. The mixture was stirred slowly for 5 min and then an aqueous solution of ascorbic acid (0.15 M, 0.1 mL) introduced. The mixture was gently shaken and the resulting solution incubated at room temperature for 10 h. The solution changed from light yellow (that of K_2PtCl_4) to black, indicating that the salt was reduced to metal Pt (0). The resulted materials were collected by filtration and then re-dispersed in hot methanol, followed by centrifugal purification to remove the organic material. This procedure was repeated three times. The resulting material was investigated by SEM and TEM. The results strongly supported that Pt nanotubes were constructed. As shown in Fig. 7, a low resolution TEM image shows a tube of *ca.* 5 micrometres long with a diameter around 500 nm (Fig. 7a), whose hollow nature was clearly evidenced by its naked end through the SEM and the high resolution TEM images

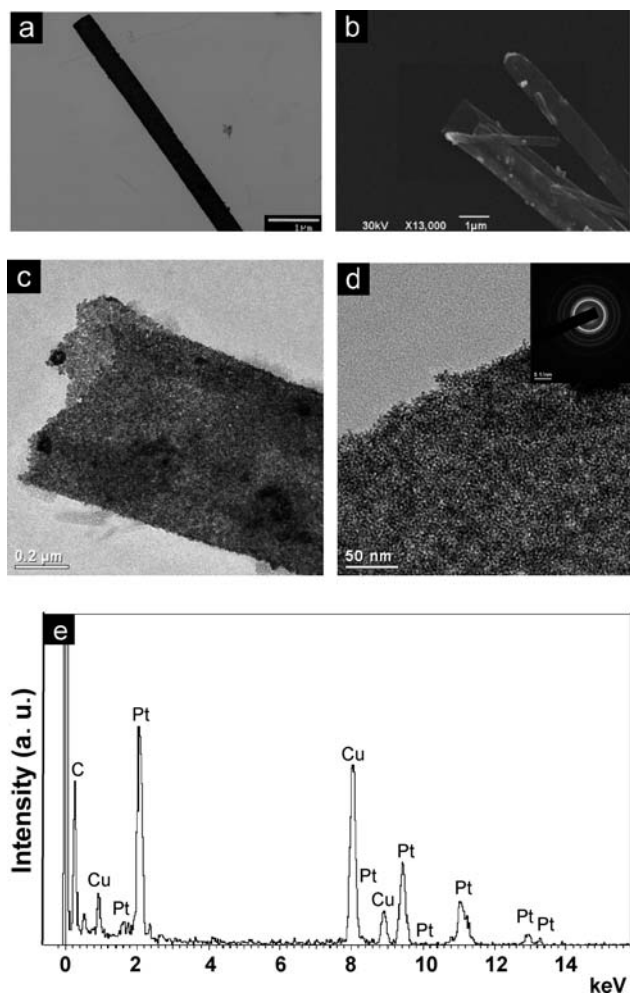


Fig. 7 (a) TEM, (b) SEM, (c) high-resolution TEM images, (d) partial magnification of image c and SAED pattern (inset), and (e) EDX diagram of Pt nanotubes, obtained on **T1** templates. The carbon and copper peaks in the EDX diagram were generated from the copper support grid.

(Fig. 7b–d). The formation of the Pt (0) metal was further confirmed by the energy dispersive X-ray (EDX) experiment, which exhibited the strong peaks of Pt (Fig. 7e). Furthermore, HR-TEM images also illustrated that the as-formed Pt nanotubes were built by Pt nanoparticles, which could be observed directly (Fig. 8d) and further confirmed to be nanocrystallites of Pt by the selected area electron diffraction (SAED) experiment (Fig. 8d, inset).³⁴ They should be formed through the reduction of Pt(II) ions on the surfaces of the organic nanotubes and then further aggregated to produce the Pt tubes.

As expected, when the spherical templates were used (a 0.1 mM solution of **T1** in methanol was employed here) and the above procedure was followed, Pt nanospheres could also be generated. Again, SEM and TEM images revealed that congregated Pt nanospheres were produced (Fig. 8a and 8b). This as-prepared product was also investigated by HRTEM image (Fig. 8c and 8d). The dark edge and pale centre in the HRTEM image of the spheres indicated that the spherical structures were also hollow, and the magnified part clearly showed Pt nanoparticles again by which the Pt sphere were constructed, while the

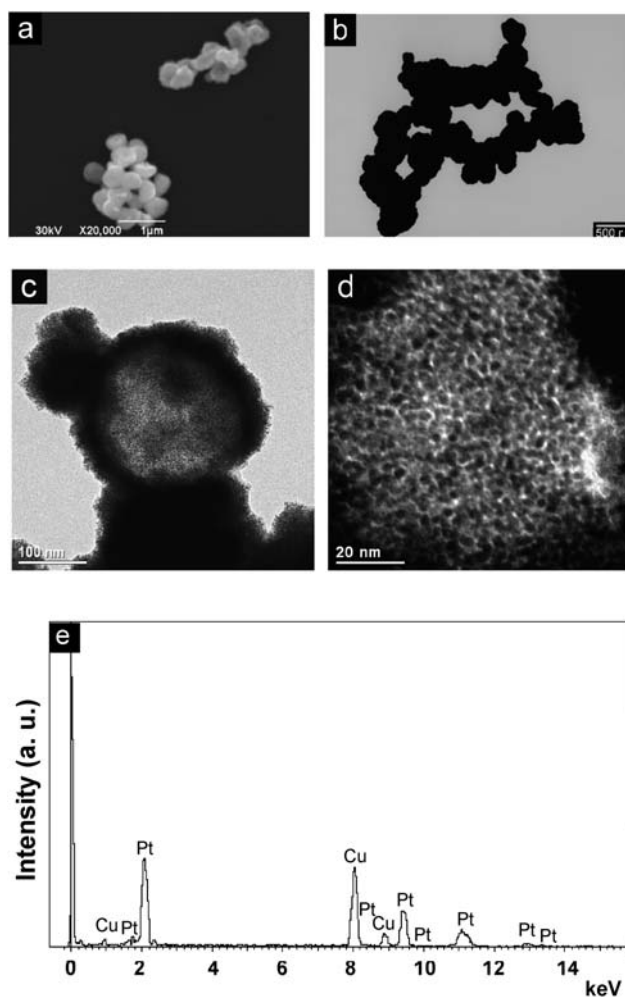


Fig. 8 (a) SEM, (b) TEM (c) high-resolution TEM images (d) partial magnification of image c and (e) EDX diagram of the as-prepared Pt spheres with **T1** as template.

EDX diagram supported that these hollow nanospheres consisted of Pt metal (Fig. 8e).

The templating effect of **T3** was also investigated. Both Pt nanotubes and nanospheres were observed when the above procedures were carried out with this compound. Because the introduction of aqueous K_2PtCl_4 partially destroyed the well-ordered tubular or vesicular structures of **T3** in methanol, the resulting Pt nanotubes and nanospheres were always accompanied by Pt agglomeration (Fig. S11 of ESI†).

Conclusions

In this study, we describe a novel class of aromatic amides that are capable of self-assembling into vesicles or micro/nano-tubes. The shape and size of the aggregates can be tuned by changing the polarity of the solvents and the concentration. The vesicle-to-tube transformation represents a new promising strategy for the construction of well-ordered supramolecular systems of different shape and size from single molecular building block. By taking advantage of simple surface chemistry, we also demonstrate that these organic micro/nano-tubes and vesicles can be used as degradable supporting materials to fabricate Pt tubes and hollow Pt spheres. This strategy provides an alternative method to prepare well-defined metal nanostructures in desired morphologies, which may be applicable to the fabrication of other transition metal nanostructures.

Acknowledgements

This research is supported by the National Science Foundation of China (Nos. 20621062, 20672137, 20732007, 20872167), the National Basic Research Program (2007CB808000) and the Science and Technology Commission of Shanghai Municipality (09XD1405300).

References

- G. M. Whitesides, J. P. Mathias and C. T. Seto, *Science*, 1991, **254**, 1312–1319.
- V. Palermo and P. Samori, *Angew. Chem., Int. Ed.*, 2007, **46**, 4428–4432.
- S. H. Seo, J. Y. Chang and G. N. Tew, *Angew. Chem., Int. Ed.*, 2006, **45**, 7526–7530.
- Y. J. Jeon, P. K. Bharadwaj, S. Choi, J. W. Lee and K. Kim, *Angew. Chem., Int. Ed.*, 2002, **41**, 4474–4476.
- P. Falvey, C. W. Lim, R. Darcy, T. Revermann, U. Karst, M. Giesbers, A. T. M. Marcelis, A. Lazar, A. W. Coleman, D. N. Reinhoudt and B. J. Ravoo, *Chem.–Eur. J.*, 2005, **11**, 1171–1180.
- B. J. Ravoo and R. Darcy, *Angew. Chem., Int. Ed.*, 2000, **39**, 4324–4326.
- F. J. M. Hoeben, I. O. Shklyarevskiy, M. J. Pouderoijen, H. Engelkamp, A. P. H. J. Schenning, P. C. M. Christianen, J. C. Maan and E. W. Meijer, *Angew. Chem., Int. Ed.*, 2006, **45**, 1232–1236.
- X. Zhang, X. Zhang, W. Shi, X. Meng, C. Lee and S. Lee, *Angew. Chem., Int. Ed.*, 2007, **46**, 1525–1528.
- Y. S. Zhao, W. Yang, D. Xiao, X. Sheng, X. Yang, Z. Shuai, Y. Luo and J. Yao, *Chem. Mater.*, 2005, **17**, 6430–6435.
- S. Hecht and A. Khan, *Angew. Chem., Int. Ed.*, 2003, **42**, 6021–6024.
- Z. Wang, C. J. Medforth and J. A. Shelnutz, *J. Am. Chem. Soc.*, 2004, **126**, 15954–15955.
- G. D. Pantos, J.-L. Wietor and J. K. M. Sanders, *Angew. Chem., Int. Ed.*, 2007, **46**, 2238–2240.
- Y. Che, A. Datar, K. Balakrishnan and L. Zang, *J. Am. Chem. Soc.*, 2007, **129**, 7234–7235.
- Z.-Y. Xiao, X. Zhao, X.-K. Jiang and Z.-T. Li, *Org. Biomol. Chem.*, 2009, **7**, 2540–2547.
- S. J. Lee, J. T. Hupp and S. T. Nguyen, *J. Am. Chem. Soc.*, 2008, **130**, 9632–9633.
- K. Balakrishnan, A. Datar, W. Zhang, X. Yang, T. Naddo, J. Huang, J. Zuo, M. Yen, J. S. Moore and L. Zang, *J. Am. Chem. Soc.*, 2006, **128**, 6576–6577.
- K. Balakrishnan, A. Datar, R. Oitker, H. Chen, J. Zuo and L. Zang, *J. Am. Chem. Soc.*, 2005, **127**, 10496–10497.
- Z. Tian, Y. Chen, W. Yang, J. Yao, L. Zhu and Z. Shuai, *Angew. Chem., Int. Ed.*, 2004, **43**, 4060–4063.
- Y. Wang, H. Fu, A. Peng, Y. Zhao, J. Ma, Y. Ma and J. Yao, *Chem. Commun.*, 2007, 1623–1625.
- B.-S. Kim, D.-J. Hong, J. Bae and M. Lee, *J. Am. Chem. Soc.*, 2005, **127**, 16333–16337.
- M. Lee, S.-J. Lee and L.-H. Jiang, *J. Am. Chem. Soc.*, 2004, **126**, 12724–12725.
- S. Burghardt, A. Hirsch, B. Schade, K. Ludwig and C. Bottcher, *Angew. Chem., Int. Ed.*, 2005, **44**, 2976–2979.
- Y. Li, B. S. Lokitz and C. L. McCormick, *Angew. Chem., Int. Ed.*, 2006, **45**, 5792–5795.
- L. Gao, L. Shi, W. Zhang, Y. An, Z. Liu, G. Li and Q. Meng, *Macromolecules*, 2005, **38**, 4548–4550.
- A. Ajayaghosh, R. Varghese, V. K. Praveen and S. Mahesh, *Angew. Chem., Int. Ed.*, 2006, **45**, 3261–3264.
- Y. Chen, B. Zhu, F. Zhang, Y. Han and Z. Bo, *Angew. Chem., Int. Ed.*, 2008, **47**, 6015–6018.
- S. Y. Kim, K. E. Lee, S. S. Han and B. Jeong, *J. Phys. Chem. B*, 2008, **112**, 7420–7423.
- B. Guan, M. Jiang, X. Yang, Q. Liang and Y. Chen, *Soft Matter*, 2008, **4**, 1393–1395.
- C. Ott, R. Hoogenboom, S. Hoepfener, D. Wouters, J.-F. Gohy and U. S. Schubert, *Soft Matter*, 2009, **5**, 84–91.
- Y. Ding, A. Mathur, M. Chen and J. Erlebacher, *Angew. Chem., Int. Ed.*, 2005, **44**, 4002–4006.
- Z. Chen, M. Waje, W. Li and Y. Yan, *Angew. Chem., Int. Ed.*, 2007, **46**, 4060–4063.
- C. Mu, Y. Yu, R. Wang, K. Wu, D. Xu and G. Guo, *Adv. Mater.*, 2004, **16**, 1550–1553.
- A. Takai, Y. Yamauchi and K. Kuroda, *Chem. Commun.*, 2008, 4171–4173.
- B. Mayers, X. Jiang, D. Sunderland, B. Cattle and Y. Xia, *J. Am. Chem. Soc.*, 2003, **125**, 13364–13365.
- S. Guo, S. Dong and E. Wang, *Chem.–Eur. J.*, 2008, **14**, 4689–4695.
- For examples fabricating Pt nanotubes from organic templates, see (a) L. Yu, I. A. Banerjee and H. Matsui, *J. Mater. Chem.*, 2004, **14**, 739–743; (b) T. Kijima, T. Yoshimura, M. Uota, T. Ikeda, D. Fujikawa, S. Mouri and S. Uoyama, *Angew. Chem., Int. Ed.*, 2004, **43**, 228–232.
- Y.-X. Gu, G.-T. Wang, X. Zhao, X.-K. Jiang and Z.-T. Li, *Langmuir*, 2009, **25**, 2684–2688.
- F. M. Menger and K. D. Gabrielson, *Angew. Chem., Int. Ed. Engl.*, 1995, **34**, 2091–2106.
- S. Takeoka, K. Mori, H. Ohkawa, K. Sou and E. Tsuchida, *J. Am. Chem. Soc.*, 2000, **122**, 7927–7935.
- H. H. Zepik, P. Walde and T. Ishikawa, *Angew. Chem., Int. Ed.*, 2008, **47**, 1323–1325.
- D. E. Discher and A. Eisenberg, *Science*, 2002, **297**, 967–973, and references therein.
- J. Du, Y. Tang, A. L. Lewis and S. P. Armes, *J. Am. Chem. Soc.*, 2005, **127**, 17982–17983.
- W. Cai, G.-T. Wang, Y.-X. Xu, X.-K. Jiang and Z.-T. Li, *J. Am. Chem. Soc.*, 2008, **130**, 6936–6937.
- A. Ajayaghosh, R. Varghese, S. Mahash and V. K. Praveen, *Angew. Chem., Int. Ed.*, 2006, **45**, 7729–7732.
- A. Ajayaghosh, P. Chithra and R. Varghese, *Angew. Chem., Int. Ed.*, 2007, **46**, 230–233.
- X. Yan, Y. Cui, Q. He, K. Wang, J. Li, W. Mu, B. Wang and Z. Ou-yang, *Chem.–Eur. J.*, 2008, **14**, 5974–5980.
- X. Yan, Q. He, K. Wang, L. Duan, Y. Cui and J. Li, *Angew. Chem., Int. Ed.*, 2007, **46**, 2431–2434.
- Y. Song, S. R. Challa, C. J. Medforth, Y. Qiu, R. K. Watt, D. Pena, J. E. Miller, F. van Swol and J. A. Shelnutz, *Chem. Commun.*, 2004, 1044–1045.
- M. Yang, W. Wang, F. Yuan, X. Zhang, J. Li, F. Liang, B. He, B. Minch and G. Wegner, *J. Am. Chem. Soc.*, 2005, **127**, 15107–15111.

-
- 50 D. Xie, M. Jiang, G. Zhang and D. Chen, *Chem.–Eur. J.*, 2007, **13**, 3346–3353.
- 51 J. L. Flippen-Anderson, J. R. Deschamps, R. D. Gilardi and C. George, *Cryst. Eng.*, 2001, **4**, 131–139.
- 52 Y. Yang, J.-F. Xiang and C.-F. Chen, *Org. Lett.*, 2007, **9**, 4355–4357.
- 53 S. J. Lee, J. T. Hupp and S. T. Nguyen, *J. Am. Chem. Soc.*, 2008, **130**, 9632–9633.
- 54 P. Tsiveriotis and N. Hadjiliadis, *Coord. Chem. Rev.*, 1999, **190–192**, 171–184.
- 55 Y.-X. Xu, X. Zhao, X.-K. Jiang and Z.-T. Li, *Chem. Commun.*, 2009, 4212–4214.